Cancer Epidemiology 60 (2019) 67–76

Contents lists available at ScienceDirect

Cancer Epidemiology

journal homepage: www.elsevier.com/locate/canep

A panel of three plasma microRNAs for colorectal cancer diagnosis

Yan Tan[a,1], Juan-Juan Lin[b,1], XiaoFei Yang[b], De-Ming Gou[c], LiWu Fu[d], Fu-Rong Li[b,*], Xiao-Fang Yu[a,**]

[a] Department of Surgery, The Second Clinical Medical College (Shenzhen People's Hospital), Jinan University, Shenzhen, China
[b] Translational Medicine Collaborative Innovation Center, The Second Clinical Medical College (Shenzhen People's Hospital), Jinan University, Shenzhen, China
[c] Shenzhen Key Laboratory of Microbial Genetic Engineering, College of Life Sciences, Shenzhen University, Shenzhen, China
[d] Collaborative Innovation Center for Cancer Medicine, State Key Laboratory of Oncology in South China, Sun Yat-Sen University Cancer Center, Guangzhou, China

ARTICLE INFO

Keywords:
microRNAs
Colorectal cancer
Diagnosis
S-poly(T) PCR
Bioinformatics

ABSTRACT

Background: Differential microRNA (miRNA) expression profiles in plasma or serum were identified, providing foundation for studying their potentially diagnostic role in colorectal cancer (CRC).

Methods: We performed S-poly(T) Plus PCR assay to select and validate differentially expressed plasma miRNAs from a sample set including 101 CRC patients, 20 patients with colorectal noncancerous polyps (NCP), and 134 healthy controls. And bioinformatics methods was used to integrated predicted or validated targets of the differentially dysregulated miRNAs and analyzed their overrepresented pathways.

Results: After the two-phase selection and validation process, we identified a miRNA panel (miR-144-3p, miR-425-5p, and miR-1260b) with high diagnostic efficiency for CRC; the panel distinguished CRC patients from controls with 93.8% sensitivity and 91.3% specificity. Results indicated that the dysregulated miRNAs in CRC were functionally involved in several key cancer-related pathways, such as axonal guidance, PI3K, and calcium signaling pathways.

Conclusions: Our study demonstrated that a plasma 3-miRNA panel may serve as a novel noninvasive biomarker to diagnose CRC. This plasma 3-miRNA panel may be related to CRC development. However, further studies are needed to highlight its theoretical strengths.

1. Introduction

Colorectal cancer (CRC) is the third most commonly diagnosed malignancy and the fourth leading cause of cancer-related deaths in the world, and its burden is expected to increase by 60% to more than 2.2 million new cases and 1.1 million cancer deaths by 2030 [1]. The 5-year survival rate is 90.3% for patients diagnosed at an early stage but that rate decreases to 12.5% for patients diagnosed in advanced stages [2]. To date, several accepted diagnostic tools for CRC, such as fecal occult blood test (FOBT), stool DNA test, computed tomography (CT), and colonoscopy, are available. However, the invasive, unpleasant, and inconvenient nature of the current diagnostic procedures limits their application [3]. Carcinoembryonic antigen (CEA) has been applied as a serum marker for CRC screening and prognosis [4,5], but CEA testing exhibits relatively low sensitivity and specificity and is thus inappropriate for screening large asymptomatic patients. Therefore, detection of CRC is challenging owing to the lack of a specific non-invasive markers. The discovery of microRNAs (miRNAs) found in plasma or serum has opened a new pathway for diagnosing CRC.

miRNAs are small noncoding (19–25 nucleotides in length), endogenous, and single-stranded RNAs that play important roles in regulating gene expression; they are also associated with numerous important pathways, including developmental and oncogenic pathways [6]. Several recent studies indicated differential CRC miRNA expression profiles in plasma or serum versus healthy individuals, such as miR-141, miR-21, miR-142-3p, miR-26a-5p, miR-1914*, and miR-1915 [7–10], which provide the foundation for studying the potentially diagnostic roles of miRNAs in CRC.

Genome-wide miRNA and mRNA expression analyses have been used to identify the functional involvement of miRNAs in the

* Corresponding author at: Translational Medicine Collaborative Innovation Center, The Second Clinical Medical College (Shenzhen People's Hospital), Jinan University, No. 1017 Dongmen North Road, Shenzhen, Guangdong, 518020, China.
** Corresponding author at: Department of Surgery, The Second Clinical Medical College (Shenzhen People's Hospital), Jinan University, No. 1017 Dongmen North Road, Shenzhen, Guangdong, 518020, China.
E-mail addresses: frli62@163.com (F.-R. Li), yuxfshui@hotmail.com (X.-F. Yu).
[1] Contributed equally.

https://doi.org/10.1016/j.canep.2019.01.015
Received 9 May 2018; Received in revised form 21 January 2019; Accepted 25 January 2019
Available online 27 March 2019
1877-7821/

progression of cancers [11]. Possible miRNA–mRNA interactions can be predicted using new computer algorithms and techniques [12–14], which enabled detailed analysis and prediction [15] and improved knowledge on cancer development and pathogenesis.

Currently, two major qPCR-based tools are used for miRNA quantification assay, namely, the poly(A) [16–19] and stem-loop methods [20–22]. Although the poly(A) method can determine miRNA expression in a high-throughput manner, the approach is less specific than others due to the nonspecific reverse transcription (RT). The stem-loop method requires individual miRNA-specific hydrolytic Taqman probes and is thus too costly for high-throughput miRNA expression profiling [23]. Moreover, given the limited number (usually six) of bases guiding the binding of the 3′ end of the step-loop primer to the target miRNAs, the efficiency of the stem-loop method is relatively low even with a pulse RT reaction [21]. In the present study, we first performed a powerful qPCR-based assay, the S-Poly(T) Plus real-time PCR assay, which exhibits superior sensitivity, specificity, and efficiency [24], to select and validate differentially expressed plasma miRNAs from a sample set including 101 CRC patients, 20 patients with colorectal noncancerous polyps (NCP), and 134 healthy controls. After the two-phase selection and validation process, we identified a miRNA panel (miR-144-3p, miR-425-5p, and miR-1260b) with high CRC diagnostic efficiency. Furthermore, we integrated predicted or validated targets of the three miRNAs and analyzed their overrepresented pathways by using Kyoto Encyclopedia of Genes and Genomes (KEGG) and Reactome database. Therefore, we demonstrated a plasma 3-miRNA panel that may serve as novel noninvasive biomarker to diagnose CRC and may be related to CRC development.

2. Materials and methods

2.1. Patients and control subjects

This study was approved by the Institutional Ethics Committees at Shenzhen People's Hospital (Shenzhen, China) and Sun Yat-sen University Cancer Center, and written informed consent was obtained from all study participants. A total of 255 participants were enrolled at the Shenzhen People's Hospital and Sun Yat-sen University Cancer Center from October 2014 to December 2015, including 101 CRC patients, 20 patients with NCP, and 134 healthy controls. The subjects in this study were newly diagnosed with CRC or NCP prior to receiving any treatments. Histological typing was performed according to the World Health Organization criteria. Staging was confirmed according to the tumor–node–metastasis (TNM) staging system. For the selection of the samples in the healthy controls, we used asymptomatic and apparently healthy volunteers without a previous history of cancer or other benign diseases. These healthy controls were matched to the CRC patients according to age and gender. The clinical characteristics of the study subjects are presented in Table 1. No significant difference was observed in the distribution of age and sex between the screening and validation datasets for both healthy and CRC groups ($P > 0.05$). Overall, 62.4% (63/101) of the patients were diagnosed with stages I–II CRC, while 37.6% (38/101) of the patients presented stage II–IV. All CRC cases in this study were adenocarcinomas.

2.2. Study guideline

A three-phase case-control test was designed to identify plasma miRNAs as potential markers for CRC (Fig. 1).

First screening phase: 485 blood-derived miRNAs were profiled in the plasma samples containing 53 CRC patients and 87 matched healthy controls, of which, 372 miRNAs that can be detected in human serum or plasma were obtained from QIAGEN website (http://www.sabiosciences.com/genetable.php?pcatn=MIHS-3106Z); 113 other blood-derived miRNAs were obtained from literatures with the key words "microRNA/miRNA", "serum/plasma/blood" in combination with "human/hsa-". From the differentially expressed miRNAs, 16 significantly altered miRNAs with P value < 0.05, fold change (FC) > 1.5 or < − 3, and cycle threshold (Ct) < 35 were identified as candidates for further testing using S-poly(T) Plus real-time PCR.

Second screening phase: We divided the 53 CRC patients into two groups as follows: 33 patients with stage I–II CRC (Group 1), 20 patients with stage III–IV CRC (Group 2). The 16 candidate miRNAs were tested in three plasma groups from the above two CRC groups and the group with 87 healthy controls with S-poly(T) Plus real-time PCR. A total of nine candidates, which were significantly altered in all three groups, were selected for further detection in the validation phase.

Validation phase: The night-candidate miRNAs discovered via the two-phase screening process were validated in additional 48 CRC patients, 20 patients with NCP, and 47 healthy controls. These 115 study subjects were used as the validation set to construct the diagnostic miRNA panel based on the logistic regression model for the differentiation of CRC patients and healthy controls. In addition, the miRNA panel was further investigated by identified their predicted or validated targets and analyzing their overrepresented pathways using KEGG and Reactome database.

Table 1
Demographic and clinical characteristics of CRC patients and healthy controls.

Variable	Screening set	Validation set	*P* Value[1]
Healthy count (%)			
Age(years)			> 0.05
Mean ± SD	59.02 ± 13.2	59.56 ± 13.9	
Range	24–88	27–78	
Gender			> 0.05
Male	44(50.6)	31(66.0)	
Female	43(49.4)	16(34.0)	
CRC count (%)			
Age(years)			> 0.05
Mean ± SD	61.02 ± 12.9	60.94 ± 14.1	
Range	26–87	26–81	
Gender			> 0.05
Female	27(50.9)	31(64.6)	
Male	26(49.1)	17(35.4)	
Location			
Colon	25(47.2)	30(62.5)	
Rectum	28(52.8)	18(37.5)	
Size			
< 5cm	37(69.8)	35(72.9)	
≥5cm	16(30.2)	13(27.1)	
Lymphatic Metastasis			
Y	22(41.5)	17(35.4)	
N	31(58.5)	31(64.6)	
Distant Metastasis			
Y	3(5.7)	3(6.3)	
N	50(94.3)	45(93.8)	
FOBT			
Y	26(49.1)	15(31.3)	
N	27(50.9)	33(68.7)	
TNM Stage			
I-II	33(62.2)	30(62.5)	
III-IV	20(37.8)	18(37.5)	
Healthy versus CRC (*P* value[2])			
Age(years)	> 0.05	> 0.05	
Gender	> 0.05	> 0.05	

[1] Significant difference between the screening and validation datasets. [2] Significant difference between the CRC and healthy dataset. Statistical comparison was performed by using two-sided Student's *t*-test or Chi-square test.

2.3. Plasma collection and RNA extraction

For the plasma preparation, peripheral blood (4 mL), which have been taken before surgery, was drawn using the standardized phlebotomy procedures into EDTA–K2 tubes (BD, Franklin Lakes, New Jersey, USA). Within 2 h, the tubes were subjected to centrifugation at 3000 *g* for 10 min at 4 °C. Subsequently, the plasma was transferred to

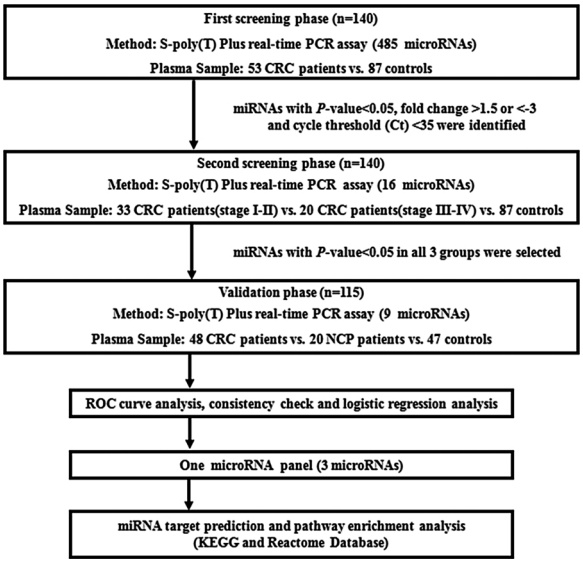

Fig. 1. Overview of the design strategy. In the screening phases, we screened the expression levels of 485 blood-derived miRNAs in the plasma samples, including 53 CRC patients and 87 healthy controls, by using the S-poly(T) Plus real-time PCR. Subsequently, the significantly altered miRNAs were validated in another independent sample set consisting of 48 CRC patients, 20 patients with NCP, and 47 healthy controls. Finally, the refined panel of plasma miRNAs selected as the CRC signature was further investigated by predicting predicted or validated targets and analyzing overrepresented pathways by using KEGG and Reactome database.

fresh tubes and stored at −80 °C until use.

Total RNA was extracted from the plasma samples by using the RNAiso Plus kit according to the manufacturer's instructions (Takara, Dalian, China). For normalizing sample-to-sample variation in the RNA extraction and as internal control, 0.1 pM spiked-in *Caenorhabditis elegans* cel-miR-54-5p was added to each denatured sample in equal amounts. RNA concentration was quantified by a NanoDrop-1000 spectrophotometer (NanoDrop-1000 Technologies, Waltham, MA).

2.4. S-poly(T) plus real-time PCR assay

Polyadenylation and RT procedures were carried out in a single step with an optimized buffer exactly according to S-Poly(T) Plus protocol [24]. For effective miRNA detection, every 7 out of the 485 miRNAs, as well as spiked-in cel-miR-54, were grouped together for the one-step polyadenylation reaction and RT. Simultaneously, miRNAs with identical forward primers or more than five base-pairings between the forward and RT primers were avoided in the same group. Thus, the following components were added to 10 μL of the reaction mixture: 1–100 ng of the total RNA from plasma samples, 2.5 μL of 4× reaction buffer mixture consists of ATP and dNTPs, 1 μL of 10× miRNA RT primer, and 1 μL of polyA/RT Enzymer mixture; in addition, variable volume of RNase-free water was also added to increase the reaction mixture to 10 μL. The reaction was carried out at 37 °C for 30 min and 42 °C for 30 min and then terminated at 75 °C for 5 min. All sequences, primers, and probes were listed in the Table S1.

Real-time PCR was performed with miRNA qPCR-assay kit (Geneup, Shenzhen, China) according to the instruction. The 20 μL of mixture consisted of the following components: 5 μL of 4 × PCR buffer, 0.4 μL of HotStar Sm-Taq Polymerase (Geneup, Shenzhen, China), 0.2 μL of 100 × Rox Reference Dye, 1 μL of 20 × probe & miRNA PCR/primer, and 1 μL of cDNA; in addition, variable volume of RNase-free water was also added to increase the reaction mixture to 20 μL. Real-time PCR was performed under the following conditions: 95 °C for 3 min, followed by 40 cycles of 95 °C for 10 s and 60 °C for 30 s. All reactions were performed in duplicate by using ABI Step One Plus Thermal Cycler. The miRNA expression level was normalized to spiked-in cel-miR-54-5p. miRNAs that showed Ct values above 35 were discarded for further analysis.

2.5. miRNAs target prediction and pathway enrichment analysis

To identify the functional involvement of miRNAs in the progression of CRC, we predicted a list of putative miRNA interacting targets in seven miRNA target prediction algorithms, namely, DIANA-microT, miRanda, mirBridge, PicTar, PITA, RNA22, and TargetScan, and two other databases, namely, TCGA (http://cancergenome.nih.gov/) and CTD (http://ctdbase.org/). Then, the predicted or validated target lists were used for pathway enrichment analysis (http://david.abcc.ncifcrf.gov/home.jsp). Differentially expressed genes were selected with P value < 0.01. KEGG pathway map (http://www.genome.jp/kegg/pathway.html) and Reactome pathway database (http://www.reactome.org/) were used to generate miRNA–mRNA interaction network and pathway enrichment analysis.

2.6. Statistics

For the quantitative RT-PCR, FCs of miRNAs were calculated by using the $2^{-\Delta\Delta Ct}$ method. Delta Ct (ΔCt) value was used to represent the individual microRNA expression level. The ΔCt of the microRNA was calculated by subtracting the Ct value of the endogenous control cel-miR-54-5p. The area under the curve (AUC) of the individual miRNA was obtained by analyzing the receiver operating characteristic (ROC) curve, which was used to evaluate the sensitivity, specificity, and corresponding cutoff values of each miRNA. Logistic regression was used to identify a panel that can distinguish CRC from healthy controls with the highest sensitivity and specificity. Consistency check was used to identify a good agreement between miRNAs and the golden standard, that is, paraffin pathology diagnosis. Statistical analysis was performed using two-tailed Student's t-test or one-way ANOVA by using the GraphPad Prism 5. Data were present as means ± SD. $P < 0.05$ was considered statistically significant. Mean value was calculated using the SPSS software version 19.0 (SPSS Inc. Chicago, IL, USA).

3. Results

3.1. Candidate miRNAs selection

To identify the profile of plasma miRNAs as a CRC fingerprint, 485 blood-derived miRNAs were examined in plasma samples of both 53 CRC patients and 87 matched healthy controls (first screening phase). Among the 485 checked miRNAs, 137 miRNAs can be readily detected in plasma with P value < 0.05 and FC > 1 or < −1 (Fig. S1 and Table S2), whereas 43 miRNAs were undetectable and 305 miRNAs showed nonlinear PCR amplification. From the differentially expressed miRNAs, a total of 16 significantly altered miRNAs with P value < 0.05, FC > 1.5 or < −3, and Ct < 35 were identified as candidates for further testing (marked in red in Table S2).

For the second screening phase, we divided the 53 CRC patients according to the TNM staging system into two groups, namely, 33 patients with stage I–II CRC (Group 1) and 20 patients with stage III–IV CRC (Group 2). The 16 candidate miRNAs were tested in the three plasma groups from the above two CRC groups and the group composed of 87 healthy controls (Table S3). A total of nine candidates, which were significantly altered in all three groups ($P < 0.05$), were selected for further detection in the validation phase (marked in red in Table S3). Out of the 9 miRNAs, 8 miRNAs, namely, miR-27a-3p, miR-143-3p, miR-144-3p, miR-148a-3p, miR-423-3p, miR-424-5p, miR-483-5p, and miR-1260b, presented significantly lower expression levels in the CRC group compared with the healthy group. By contrast, the CRC group showed significantly higher expression levels of miR-425-5p compared with the healthy group.

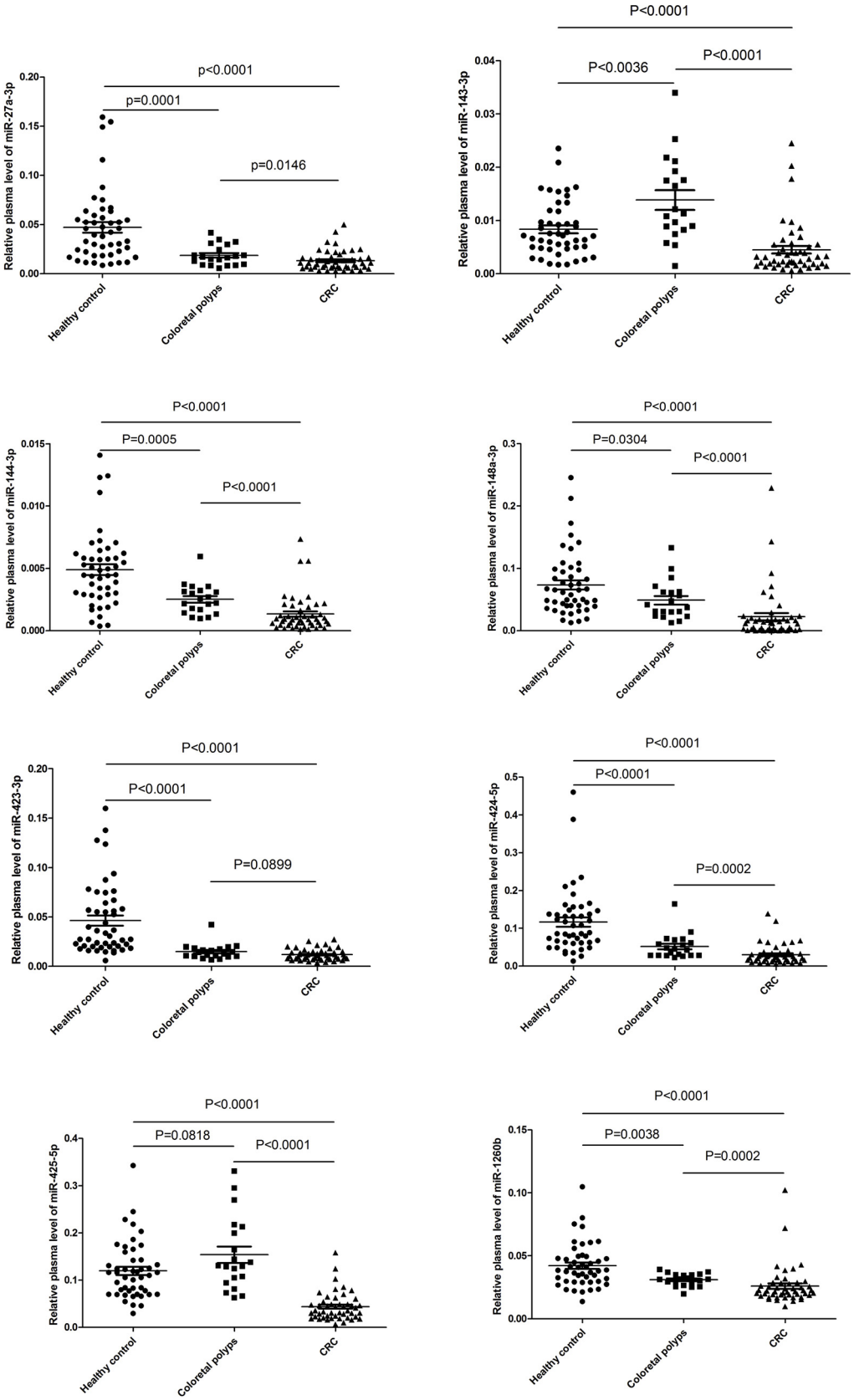

Fig. 2. Relative expression level of plasma miRNAs in the validation phase. miRNAs were quantified in the plasma of 48 CRC patients, 20 patients with NCP, and 47 healthy controls. miRNA levels were normalized to spiked-in cel-miR-54-5p and represented in scatter plots. Data are shown as mean ± SD. The longest line in the middle represents the mean value. CRC: colorectal cancer.

3.2. Validating the identified miRNAs

To verify the expression of 9 miRNAs for potential use as plasma biomarkers in CRC diagnosis, we further assessed these miRNAs in additional 48 CRC patients, 20 patients with NCP, and 47 healthy controls (validation phase). Comparison between the CRC patients group and healthy controls group was performed. The trend of miRNA expression alteration was generally concordant between the screening phases and the validation phase, and 8 out of the 9 miRNAs, except miR-483-5p ($P = 0.918$), were significantly downregulated. To determine the validity of the 8 miRNAs, we further analyzed the expression differences among the CRC patients, patients with NCP, and healthy controls. As shown in Fig. 2, five miRNAs (miR-27a-3p, miR-144-3p, miR-148a-3p, miR-424-5p, and miR-1260b) were significantly downregulated in both CRC patients and patients with NPC as compared with those in healthy controls. miR-143-3p was significantly downregulated in CRC patients and upregulated in patients with NCP compared with healthy controls. miR-425-5p did not show significantly differential expression between the patients with NCP and healthy controls ($P = 0.0818$) but was significantly downregulated in CRC patients. Considering the disability to distinguish CRC patients from the patients with NCP ($P = 0.0899$), we excluded miR-423-3p from validation miRNAs. We finally selected seven miRNAs, which were significantly down-regulated in CRC patients compared with patients with NCP and healthy controls, with considerable potential as plasma biomarkers for CRC diagnosis.

3.3. Diagnostic performance of plasma miRNAs for CRC

To investigate the diagnostic values of the seven miRNAs, we analyzed the ROC curve. All seven miRNAs showed excellent AUCs (Fig. 3A–G). The AUCs, sensitivities, and specificities are listed as follows respectively: 0.881 (95% CI: 0.816–0.946, $P < 0.05$), 75.0%, and 85.0% for miR-27a-3p; 0.777 (95% CI: 0.682–0.873, $P < 0.05$), 72.9%, and 78.7% for miR-143-3p; 0.887 (95% CI: 0.815–0.959, $P < 0.05$), 93.8%, and 78.7% for miR-144-3p; 0.871 (95% CI: 0.795–0.947, $P < 0.05$), 79.2%, and 91.5% for miR-148a-3p; 0.919 (95% CI: 0.863–0.975, $P < 0.05$), 79.2%, and 93.6% for miR-424-5p; 0.910 (95% CI: 0.852–0.969, $P < 0.05$), 83.3%, and 91.5% for miR-425-5p; and 0.848 (95% CI: 0.766–0.929, $P < 0.05$), 81.3%, and 83.3% for miR-1260b. The seven miRNAs can distinguish CRC from the healthy controls effectively. Using logistic regression, we obtained the optimal combination of miRNAs to diagnose CRC as follows: miR-144-3p, miR-425-5p, and miR-1260b. In addition, the AUC of the miRNA combination was 0.954 (95% CI: 0.914–0.994, $P < 0.05$) with 93.8% sensitivity and 91.3% specificity (Fig. 3H), showing higher diagnostic performance than CEA, CA19-9, and FOBT (Table 2). These results suggest that the panel of the three miRNAs were potential biomarkers for CRC diagnosis.

To identify if there was a good agreement between the miRNAs detected by S-poly(T) Plus real-time PCR and paraffin pathology to diagnose CRC, we performed consistency check in 48 CRC patients and 47 healthy controls by established matched fourfold table (Table S4). The consistency check results showed that the Kappa values ($P < 0.05$) for miR-27a-3p, miR-143-3p, miR-144-3p, miR-148a-3p, miR-424-5p, miR-425-5p, and miR-1260b were 0.60, 0.52, 0.73, 0.71, 0.73, 0.75, and 0.64, respectively. Thus, seven plasma miRNAs showed good agreement in CRC diagnosis relative to paraffin pathology. These plasma miRNAs may also serve as a novel noninvasive biomarker for CRC.

3.4. Relationship between plasma miRNAs expression and clinical parameters

To investigate the clinical significance of the seven plasma miRNAs, we explored the correlation of the miRNA expression levels with demographic and clinical factors using Student's *t*-test or one-way ANOVA. In this analysis, samples from the validation set were used to conduct the calculation. No obvious differences were observed when the CRC patients were stratified by age, location, tumor size, lymphatic metastasis, distant metastasis, CEA expression level, CA19-9 expression level, or TNM stage. By contrast, the expression levels of five plasma miRNAs (miR-27a-3p, miR-143-3p, miR-148a-3p, miR-424-5p, and miR-425-5p) were correlated with the gender of CRC patients ($P < 0.05$). As shown in Table S5, the expression levels of miR-27a-3p, miR-143-3p, miR-148a-3p, miR-424-5p, and miR-425-5p in 31 male cases were significantly lower than those in 17 female cases. In addition, we found that the miR-144-3p expression level in FOBT positive patients were significantly lower than those in negative patients ($P < 0.05$).

3.5. Target prediction and pathway enrichment analysis for miR-144-3p, miR-425-5p, and miR-1260b

To illustrate the impact of miRNAs involved in the pathogenesis of CRC, we conducted pathway enrichment analysis based on predicted or validated targets. We first analyzed the differential expression levels of miR-144-3p, miR-425-5p, and miR-1260b based on the miRNA data, including 270 tumor samples and 8 normal samples downloaded from TCGA database (Table S6). The significant *P* values of the three miRNAs were calculated using the *t*-test and adjusted using the Benjamini–Hochberg method. miR-1260b was significantly upregulated, whereas miR-144-3p and miR-425-5p were significantly downregulated in tumor samples compared with the normal samples (Table 3). Subsequently, we predicted a list of putative miRNA interacting targets by downloading the mRNA data containing 287 tumor samples and 41 normal samples (Table S7). The mRNA data showed 3310 significantly upregulated genes and 1793 significantly downregulated genes. miR-1260b had 53 target genes significantly downregulated in tumors, whereas miR-425-5p and miR-144-3p had respectively 159, 162 target genes significantly upregulated in tumors (Table S8). In combination with the CTD database, nine MARKER-related genes were observed in CRC, including ABCA1, ABCA8, EFEMP1, MAOB, RET, STARD8, ABCA10, LRRC3B, and SFRP1. The differentially expressed target genes and the miRNA-mRNA networks are shown in Fig. 4.

The predicted target genes were used for pathway enrichment analysis by using KEGG pathway map and Reactome pathway database. The results from pathway enrichment analysis based on predicted or validated targets from the dysregulated miRNAs revealed a number of cancer-associated pathways. The miRNA pathways were significantly enriched in the KEGG pathway, as shown in Fig. 5A. miR-144-3p was enriched in the axon guidance pathway ($P = 0.002$), whereas miR-425-5p was enriched in the calcium signaling pathway ($P = 0.000$); however, miR-1260b was not enriched in any pathway (Table 4). Numerous Reactome signal enrichment pathways in miRNAs (Table S9) were observed, but only the most significant pathways are shown in Fig. 5B. miR-144-3p was mainly enriched in the phosphoinositide 3-kinase (PI3K) and platelet-derived growth factor (PDGF) pathways ($P < 0.01$), whereas miR-425-5p was mainly enriched in the guanylate cyclase and cyclic guanosine monophosphate (cGMP) pathways ($P < 0.01$); however, miR-1260b was still not significantly enriched. These key regulators and signal transduction pathways may form feedback loops with miRNAs to modulate apoptosis, cell cycle, cell migration, and invasion in CRC development.

4. Discussion

CRC is one of the most commonly diagnosed cancers. This cancer can be prevented because most CRC cells originate from their precursor adenomatous polyps [25]. Screening mainly aims to detect the sporadic CRC cases in people aged ≥ 50 years [26]. Recently, a multitarget stool

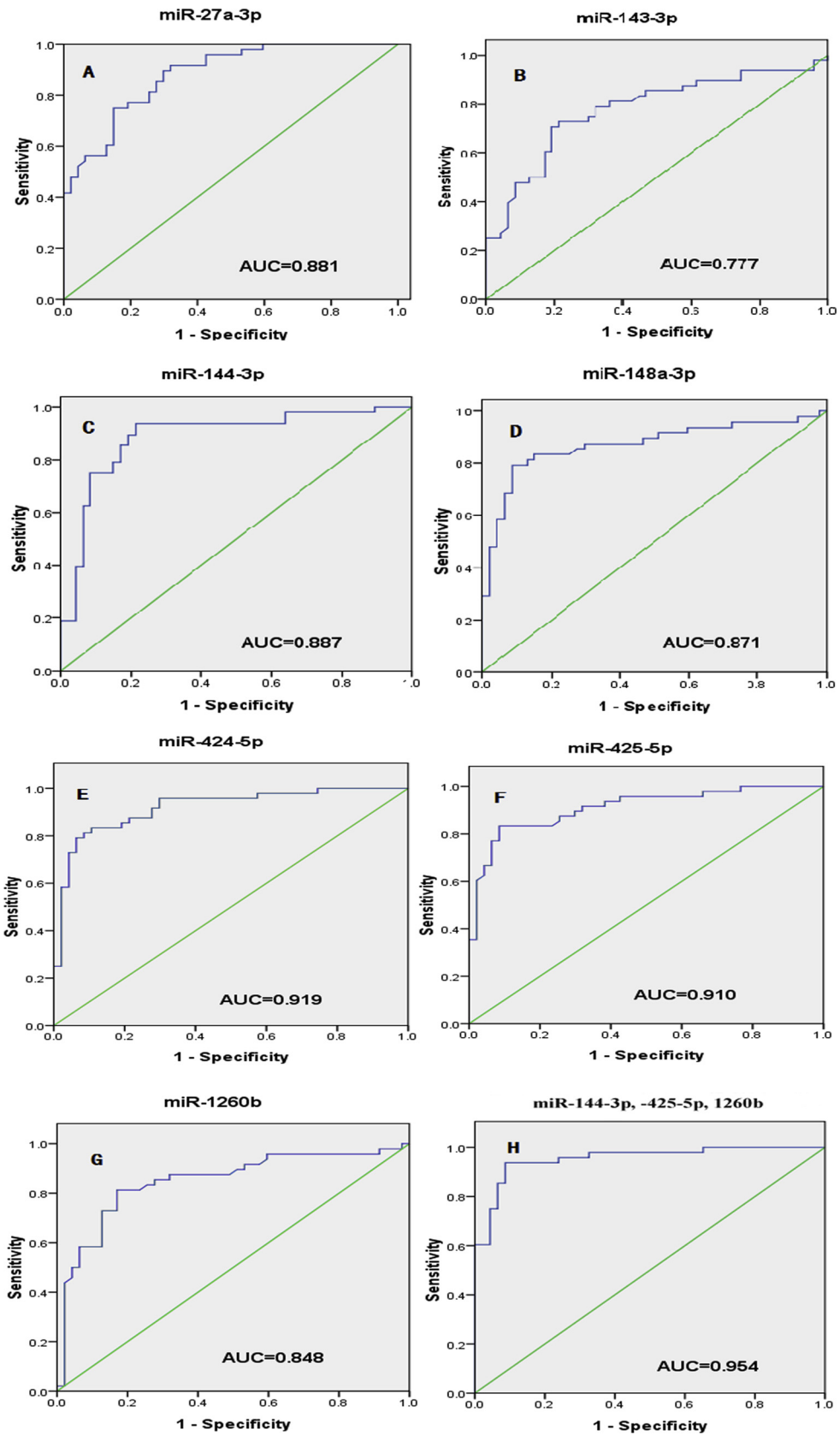

Fig. 3. ROC curve analysis for discriminating CRC from healthy controls on the validation dataset. (A–G) A total of seven miRNAs were selected from the validation set. We listed the AUCs, sensitivities, and specificities as follows: 0.881 (95% CI: 0.816–0.946, $P < 0.05$), 75.0%, and 85.0% for miR-27a-3p; 0.777 (95% CI: 0.682–0.873, $P < 0.05$), 72.9%, and 78.7% for miR-143-3p; 0.887 (95% CI: 0.815–0.959, $P < 0.05$), 93.8%, and 78.7% for miR-144-3p; 0.871 (95% CI: 0.795–0.947, $P < 0.05$), 79.2%, and 91.5% for miR-148a-3p; 0.919 (95% CI: 0.863–0.975, $P < 0.05$), 79.2%, and 93.6% for miR-424-5p; 0.910 (95% CI: 0.852–0.969, $P < 0.05$), 83.3%, and 91.5% for miR-425-5p; and 0.848 (95% CI: 0.766–0.929, $P < 0.05$), 81.3%, and 83.3% for miR-1260b. (H) The combined analysis of miR-144-3p, miR-425-5p, and miR-1260b revealed an AUC of 0.954 (95% CI: 0.914–0.994, $P < 0.05$), with 93.8% sensitivity and 91.3% specificity.

DNA test has been made commercially available in the United States. Although this test is the most sensitive noninvasive CRC screening test, further research is needed in several areas, such as cost-effectiveness of DNA stool testing in real-life populations [27]. Previous studies showed that compared with mRNA levels, miRNA analysis may be more efficient to understand the biological behavior of diseases [28,29]. Mitchell et al.confirmed the existence of abundant and stable miRNAs in plasma. miRNAs offer numerous advantages, such as excellent sensitivity and

Table 2
Diagnostic performance of biochemical indicators commonly used in CRC compared with the panel of miR-144-3p, miR-425-5p, miR-1260b.

	miR-144-3p, -425-5p, -1260b	CEA	CA19-9	FOBT
SEN	93.8%	35.4%(17/48)	22.9%(11/48)	31.3%(15/48)
SPE	91.3%	87.2%(41/47)	87.2%(41/47)	63.8%(30/47)

SEN: sensitivity; SPE: specificity.

Table 3
Differential expression of miR-144-3p, miR-425-5p, miR-1260b based on miRNAs database.

miRNA	Log2(FC)	*P*	adj. *P*
miR-144-3p	−5.49E+00	9.22E-17	9.64E-16
miR-425-5p	−9.48E-01	2.37E-03	3.07E-03
miR-1260b	2.00E+00	3.58E-09	6.71E-09

FC: fold change. adj.*P*: adjusted *P* value.

specificity, less trauma, and relatively low cost. As shown in Table 2, sensitivity and specificity of CRC detection by the panel composed of miR-144-3p, miR-425-5p, and miR-1260 are 93.8% and 91.3%, respectively, which are significantly higher than those of any single-factor index, such as CEA (35.4% sensitivity, 87.2% specificity), CA19-9 (22.9% sensitivity, 87.2% specificity), and FOBT (31.3% sensitivity, 63.8% specificity) [30].

miR-27a-3p, miR-143-3p, miR-144-3p, miR-148a-3p, miR-424-5p, miR-425-5p, and miR-1260b were significantly downregulated in the CRC plasma samples compared with the control samples. The AUC values of seven miRNAs were all above 0.7 with high sensitivity and specificity, which indicated good accuracy. The consistency check results also showed a good agreement between the miRNAs and paraffin pathology in CRC diagnosis. RUNX1 is an important transcription factor in tumorigenesis and progression, and its role may be related to p53 [31]. Studies showed that miR-27a-3p is related to RUNX1 [32–34]. Murat Kara et al. [35] found that the abnormal expression of miR-27a-3p in the CRC tissue is closely related to RUNX1, which participate in the occurrence of CRC. miR-27a-3p is also associated with breast cancer [36] and glioma [37], whereas its downregulated expression can be detected in the cerebrospinal fluid of patients with Alzheimer disease [38]. The abnormal expression of miR-143-3p in CRC participates in the regulation of several important signaling pathways by target APC, TGFβ, PI3K, and FHIT [39,40]. In addition, miR-144-3p, miR-148a-3p, miR-424-5p, and miR-425-5p [40–44] are differentially expressed in CRC. However, further studies is required to test the other types of tumors to determine whether the seven plasma miRNAs are capable of discriminating CRC from other tumors.

In the present study, we also investigated the relationship between seven plasma miRNAs and clinical parameters, suggesting that the expression level of five plasma miRNAs (miR-27a-3p, miR-143-3p, miR-148a-3p, miR-424-5p, and miR-425-5p) were correlated with the gender of the CRC patients ($P < 0.05$). In addition, the miR-144-3p expression level in FOBT-positive patients was significantly lower than that in FOBT-negative patients ($P < 0.05$). However, given that most of the patients in the validation set were diagnosed with stage II and III CRC while patients with stage I and IV were fewer, no evident differences were observed when CRC patients were stratified by TNM stage. Future studies may be necessary to compare the plasma from various stages of CRC samples with reasonable statistical estimation. TNM staging system is currently the most important tool used by clinical oncologists to estimate the tumor burden, predict prognosis and survival, and select the best combination of treatment modalities, such as surgery, radiation, and chemotherapy [45,46]; thus, plasma miRNAs

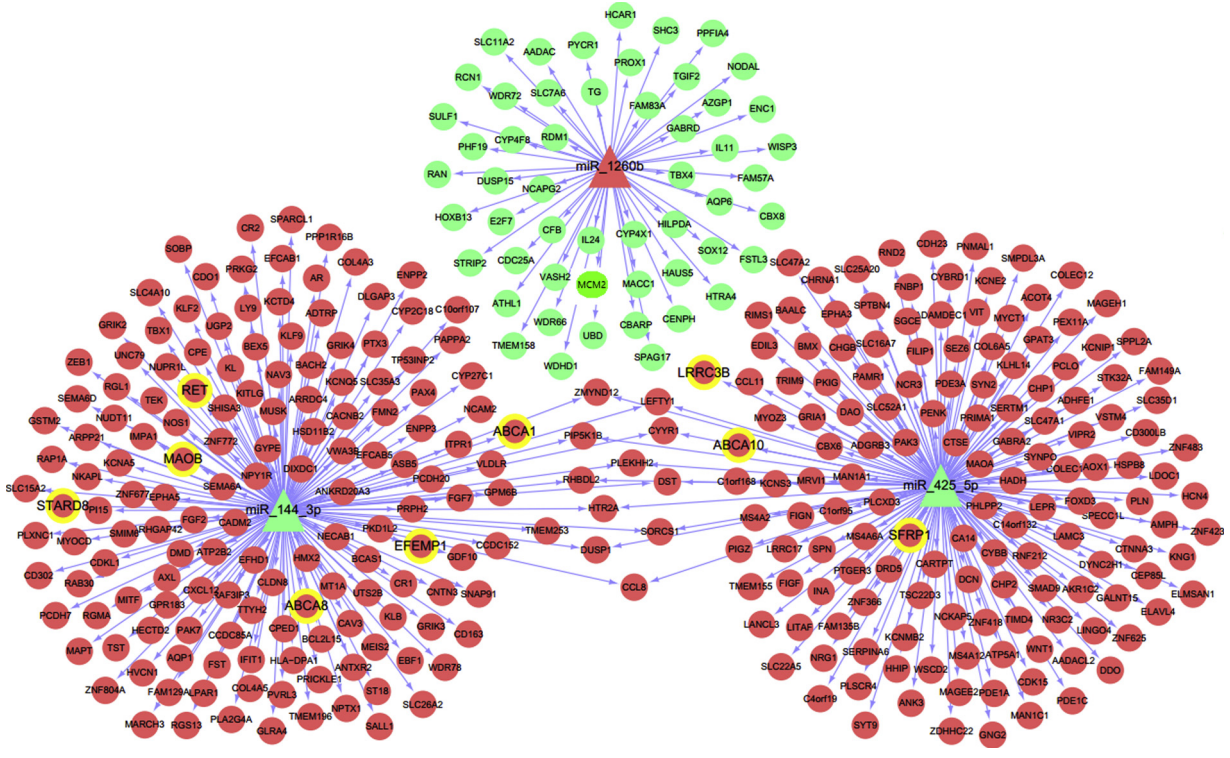

Fig. 4. Schematic of the selected miRNA–mRNA networks involved in CRC. Red indicates higher level in CRC and green represents lower level compared with controls. The triangle refers to miRNAs, and the circle refers to target genes. Yellow refers to MARKER genes related to CRC that are recruited in the CTD database. In tumors, miR-1260b possesses 53 target genes that are significantly down-regulated, whereas miR-425-5p and miR-144-3p possess 159 and 162 target genes, respectively, that were significantly upregulated. A total of nine MARKER-related genes are found in CRC, including ABCA1, ABCA8, EFEMP1, MAOB, RET, STARD8, ABCA10, LRRC3B, and SFRP1 (For interpretation of the references to colour in this figure legend, the reader is referred to the web version of this article).

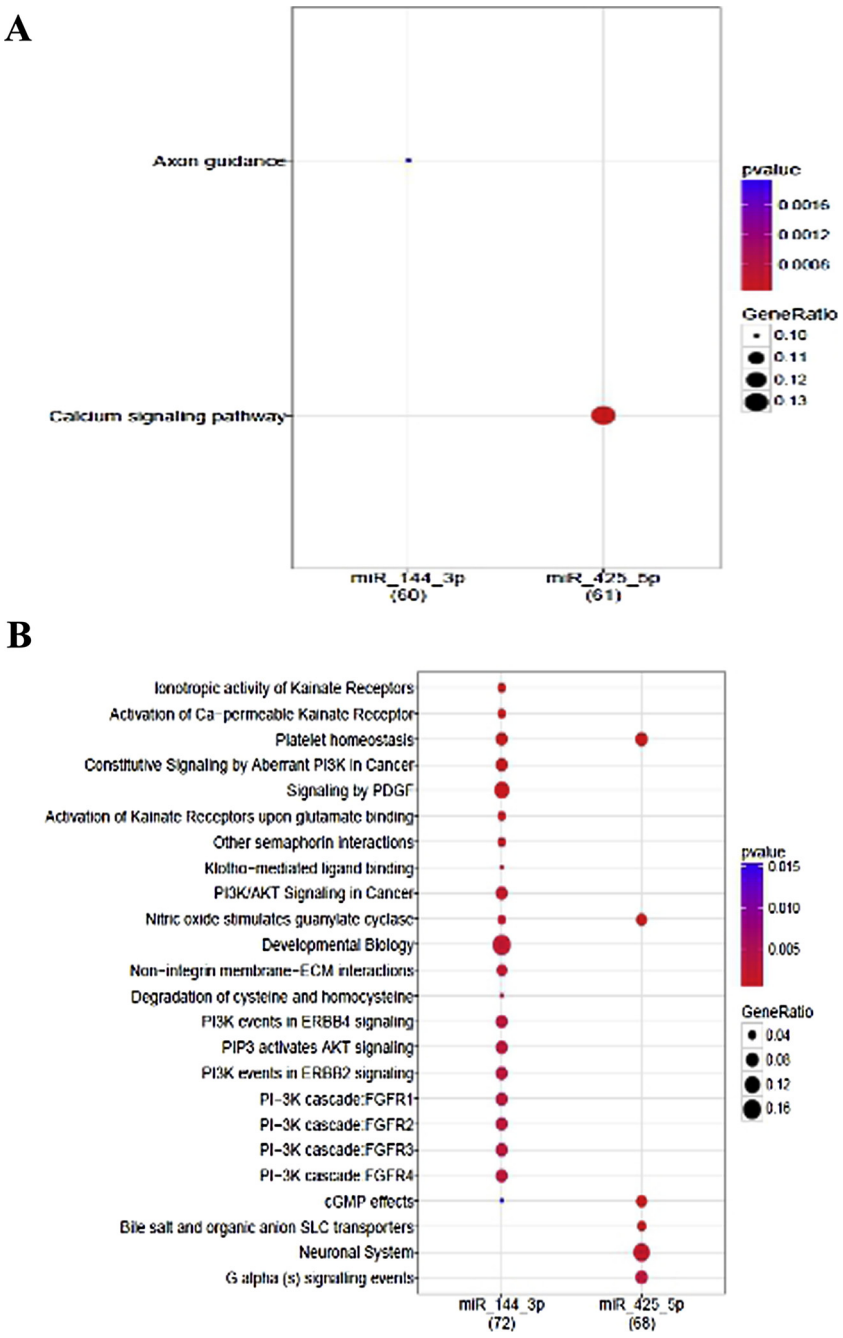

Fig. 5. (A) Over-represented KEGG pathways associated with miRNA target genes. miR-144-3p was enriched in the axon guidance pathway ($P = 0.002$), whereas miR-425-5p was enriched in the calcium signaling pathway ($P = 0.000$). (B) Overrepresented Reactome pathways associated with miRNA target genes. The most significant Reactome signal enrichment pathways are shown. The results indicate that miR-144-3p is mainly enriched in the PI3K and PDGF pathways ($P < 0.01$), whereas miR-425-5p is mainly enriched in the guanylate cyclase and cGMP pathways ($P < 0.01$).

may present an important prognostic value [47].

A miRNA can contain multiple target genes, and multiple miRNAs can also regulate the same gene; thus, miRNAs are involved in the complex gene and pathway regulations in cancers. Genome-wide miRNA and mRNA expression analyses have been used to identify the functional involvement of miRNAs in the development and pathogenesis of cancers [11]. Thus, we conducted pathway enrichment analysis based on the predicted targets and found that the dysregulated miRNAs

Table 4
Details of over-represented KEGG pathways associated with miRNA target genes.

miRNA	Description of pathway	*P*	adj. *P*	Gene count	Gene
miR-144-3p	Axon guidance	0.002	0.002	6	CXCL12/EPHA5/PAK7/PLXNC1/SEMA6A/SEMA6D
miR-425-5p	Calcium signaling pathway	0.000	0.000	8	CHP1/CHP2/DRD5/HTR2A/PLN/ PDE1A/PDE1C /PTGER3

adj. *P*:adjusted *P* value.

(miR-144-3p and miR-425-5p) in CRC were functionally involved in several key cancer-related pathways, such as axonal guidance, PI3K, cGMP, and calcium signaling pathways (Fig. 5). Wu et al. reported that the significant upregulation of miR-144-3p can inhibit the activation of PI3K signaling pathway by downregulating the expression of IRS1, which suppresses the growth and metastasis of laryngeal squamous cell carcinoma [48]. Other researchers found that miR-144-3p promotes cell proliferation, migration, and invasion in nasopharyngeal carcinoma by repressing the expression of phosphatase and tensin homolog (PTEN) to activate the PI3K pathway [49]. These results were consistent with our finding that the PI3K pathway is one of the primary signal transduction pathways in miR-144-3p to predict target genes. In addition, a large number of reports suggested that the Ca^{2+} signaling pathway played an important role in tumor occurrence and development. Tumor cells showed markedly higher Ca^{2+} concentration compared with normal cells and elevated expression levels of L-type and T-type Ca^{2+} channels [50]. miR-425-5p was mainly enriched in the Ca^{2+}, cyclic adenosine monophosphate (cAMP), and cGMP signaling pathways, indicating that the same miRNA regulates a variety of target genes. Ca^{2+}-dependent activation of adenosine 5′-monophosphate activated protein kinase (AMPK) in cancer cells causes G1-phase cell cycle arrest and enhances cell viability or survival [51].

5. Conclusions

We demonstrated that seven miRNAs may function as noninvasive biomarkers to detect CRC. The consistency check results showed good agreement between miRNAs and the golden standard paraffin pathology to diagnose CRC. In particular, the panel of three miRNAs (miR-144-3p, miR-425-5p, and miR-1260b) yielded an AUC of 0.954, with 93.8% sensitivity and 91.3% specificity, which demonstrated higher diagnostic performance compared with the single-factor index. Furthermore, miRNA target prediction and pathway enrichment analysis indicated that the dysregulated miRNAs in CRC are functionally involved in several key cancer-related pathways, such as axonal guidance, PI3K, and calcium signaling pathways. Thus, the plasma 3-miRNA panel may serve as a novel noninvasive biomarker for CRC diagnosis and may be related to CRC development. However, further studies are needed to highlight the theoretical strengths of this approach.

Authors' contributions

The experiments were designed by L.F.R. and Y.X.F., T.Y. performed the majority of the experiments and data analysis. L.J.J. assisted with data analysis and wrote the paper. Y.X.F., G.D.M., and F.L.W. provided materials and made critical suggestions during the course of this work.

Ethics approval and consent to participate

This study was approved by the Institutional Ethics Committees at Shenzhen People's Hospital (Shenzhen, China) and Sun Yat-sen University Cancer Center, and written informed consent was obtained from all study participants.

Availability of data and materials

All data generated or analyzed during this study were included in this article and its supplementary information files. And the datasets used and analyzed during the current study are available from the corresponding author on reasonable request, the TCGA dataset (http://gdac.broadinstitute.org/), and CTD dataset (http://ctdbase.org/).

Funding

This work was supported by the National Natural Science Foundation of China (No. 81502589), The Natural Science Foundation of Guangdong (No. 408140352062, 2014A030310481) and The Science and Technology Project of Shenzhen (No. CXZZ20130515092016300, JCYJ20160422 142707177).

Conflict of interest

The authors declare that they have no competing interests.

Acknowledgments

We acknowledge the contribution of the people who took part in this research, often at a time of great challenge in their lives, thank you. In addition, we thank TCGA and CTD dataset for providing data and all the patients participated in our study.

Appendix A. Supplementary data

Supplementary material related to this article can be found, in the online version, at doi:https://doi.org/10.1016/j.canep.2019.01.015.

References

[1] Melina Arnold, Global patterns and trends in colorectal cancer incidence and mortality, BMJ 66 (2017) 683–691.
[2] R. Siegel, C. Desantis, A. Jemal, Colorectal cancer statistics, CA Cancer J. Clin. 2014 (64) (2014) 104–117.
[3] S.J. Winawer, The multidisciplinary management of gastrointestinal cancer. Colorectal cancer screening, Best Pract. Res. Clin. Gastroenterol. 21 (2007) 031–1048.
[4] P. Thomas, C.A. Toth, K.S. Saini, J.M. Jessup, G. Steele Jr., The structure, metabolism and function of the carcinoembryonic antigen gene family, Biochim. Biophys. Acta 1032 (1990) 177–189.
[5] M.J. Duffy, Carcinoembryonic antigen as a marker for colorectal cancer: is it clinically useful? Clin. Chem. 47 (2001) 624–630.
[6] A. Hata, B.N. Davis, Regulation of pri-miRNA processing through Smads, Adv. Exp. Med. Biol. 700 (2010) 15–27.
[7] H. Cheng, L. Zhang, D.E. Cogdell, H. Zheng, A.J. Schetter, M. Nykter, et al., Circulating plasma MiR-141 is a novel biomarker for metastatic colon cancer and predicts poor prognosis, PLoS One 6 (2011) e17745.
[8] Y. Toiyama, M. Takahashi, K. Hur, T. Nagasaka, K. Tanaka, Y. Inoue, et al., Serum miR-21 as a diagnostic and prognostic biomarker in colorectal cancer, J. Natl. Cancer Inst. 105 (2013) 849–859.
[9] R. Ghanbari, N. Mosakhani, J. Asadi, N. Nouraee, S.J. Mowla, Y. Yazdani, et al., Downregulation of plasma MiR-142-3p and MiR-26a-5p in patients with colorectal carcinoma, Iran. J. Cancer Prev. 8 (2015) e2329.
[10] J. Hu, G. Cai, Y. Xu, S. Ca, The plasma microRNA miR-1914* and -1915 suppresses chemoresistant in colorectal cancer patients by down-regulating NFIX, Curr. Mol. Med. 16 (2016) 70–82.
[11] Y. Shao, W. Gu, Z. Ning, X. Song, H. Pei, J. Jiang, Evaluating the prognostic value of microRNA-203 in solid tumors based on a meta-analysis and the cancer genome atlas (TCGA) datasets, Cell. Physiol. Biochem. 41 (2017) 1468–1480.
[12] J. Ruan, H. Chen, L. Kurgan, K. Chen, C. Kang, Pu P. HuMiTar, A sequence-based method for prediction of human microRNA targets, Algorithms Mol. Biol. 3 (2008) 16.
[13] D. Yue, H. Liu, Y. Huang, Survey of computational algorithms for microRNA target prediction, Curr. Genomics 10 (2009) 478–492.
[14] G.L. Papadopoulos, M. Reczko, V.A. Simossis, P. Sethupathy, A.G. Hatzigeorgiou, The database of experimentally supported targets: a functional update of TarBase, Nucleic Acids Res. 37 (2009) D155–158.
[15] B.P. Lewis, I.H. Shih, M.W. Jones-Rhoades, D.P. Bartel, C.B. Burge, Prediction of mammalian microRNA targets, Cell 115 (2003) 787–798.
[16] R. Shi, V.L. Chiang, Facile means for quantifying microRNA expression by real-time PCR, Biotechniques 39 (2005) 519–525.
[17] I. Reichenstein, N. Aizenberg, M. Goshen, Z. Bentwich, Y.S. Avni, A novel qPCR assay for viral encoded microRNAs, J. Virol. Methods 163 (2010) 323–328.
[18] I. Balcells, S. Cirera, P.K. Busk, Specific and sensitive quantitative RT-PCR of miRNAs with DNA primers, BMC Biotechnol. 11 (2011) 70–81.
[19] S.G. Jensen, P. Lamy, M.H. Rasmussen, M.S. Ostenfeld, L. Dyrskjøt, T.F. Orntoft, et al., Evaluation of two commercial global miRNA expression profiling platforms for detection of less abundant miRNAs, BMC Genomics 12 (2011) 435–461.
[20] J. Feng, K. Wang, X. Liu, S. Chen, J. Chen, The quantification of tomato microRNAs response to viral infection by stem-loop real-time RT-PCR, Gene 437 (2009) 14–21.
[21] F. Tang, P. Hajkova, S.C. Barton, K. Lao, M.A. Surani, MicroRNA expression profiling of single whole embryonic stem cells, Nucleic Acids Res. 34 (2006) e9–e16.
[22] P. Mestdagh, T. Feys, N. Bernard, S. Guenther, C. Chen, Highthroughput stem-loop RT-qPCR miRNA expression profiling using minute amounts of input RNA, Nucleic Acids Res. 36 (2008) e143–151 2008.
[23] E. Varkonyi-Gasic, R. Wu, M. Wood, E.F. Walton, R.P. Hellens, Protocol. A highly

sensitive RT-PCR method for detection and quantification of microRNAs, Plant Methods 3 (2007) 12–24.
[24] Y. Niu, L. Zhang, H. Qiu, Y. Wu, Z. Wang, Y. Zai, et al., An improved method for detecting circulating microRNAs with S-poly(T) plus real-time PCR, Sci. Rep. 5 (2015) 15100.
[25] J.H. Bond, Colon polyps and cancer, Endoscopy 35 (2003) 27–35.
[26] B.W. Stewart, P. Kleihus, World Cancer Report, IARC Press, Lyon, 2003.
[27] T. Kadiyska, A. Nossikoff, Stool DNA methylation assays in colorectal cancer screening, World J. Gastroenterol. 21 (2015) 10057–10061.
[28] Y. Xi, A. Formentini, M. Chien, D.B. Weir, J.J. Russo, J. Ju, et al., Prognostic values of microRNAs in colorectal cancer, Biomark. Insights 2 (2006) 113–121.
[29] J. Lu, G. Getz, E.A. Miska, E. Alvarez-Saavedra, J. Lamb, D. Peck, et al., MicroRNA expression profles classify human cancers, Nature 435 (2005) 834–838.
[30] P.S. Mitchell, R.K. Parkin, E.M. Kroh, B.R. Fritz, S.K. Wyman, E.L. Pogosova-Agadjanyan, et al., Circulating microRNAs as stable blood-based markers for cancer detection, Proc Natl Acad Sci U S A 105 (2008) 10513–10518.
[31] Y. Ito, S.C. Bae, L.S. Chuang, The RUNX family: developmental regulators in cancer, Nat. Rev. Cancer 15 (2015) 81–95.
[32] J. Feng, A.M. Iwama, K. Kohu, MicroRNA-27 enhances differentiation of myeloblasts into granulocytes by post-transcriptionally downregulating Runx1, Br. J. Haematol. 145 (2009) 412–423.
[33] O. Ben-Ami, N. Pencovich, J. Lotem, D. Levanon, Y. Groner, A regulatory interplay between miR-27a and Runx1 during megakaryopoiesis, Proc. Natl. Acad. Sci. U. S. A. 106 (2009) 238–243.
[34] S. Rossetti, N. Sacchi, RUNX1: a MicroRNA hub in normal and malignant hematopoiesis, Int. J. Mol. Sci. 14 (2013) 1566–1588.
[35] M. Kara, O. Yumrutas, O. Ozcan, O.I. Celik, E. Bozgeyik, I. Bozgeyik, et al., Differential expressions of cancer-associated genes and their regulatory miRNAs in colorectal carcinoma, Gene 567 (2015) 81–86.
[36] C. Camps, H.K. Saini, D.R. Mole, H. Choudhry, M. Reczko, J.A. Guerra-Assunção, et al., Integrated analysis of microRNA and mRNA expression and association with HIF binding reveals the complexity of microRNA expression regulation under hypoxia, Mol. Cancer 13 (2014) 28.
[37] W. Xu, M. Liu, X. Peng, P. Zhou, J. Zhou, K. Xu, et al., miR-24-3p and miR-27a-3p promote cell proliferation in glioma cells via cooperative regulation of MXI1, Int. J. Oncol. 42 (2013) 757–766.
[38] C. Sala Frigerio, P. Lau, E. Salta, J. Tournoy, K. Bossers, R. Vandenberghe, et al., Reduced expression of hsa-miR-27a-3p in CSF of patients with Alzheimer disease, Neurology 81 (2013) 2103–2106.
[39] K. Schee, S. Lorenz, M.M. Worren, C.C. Günther, M. Holden, E. Hovig, et al., Deep sequencing the MicroRNA transcriptome in colorectal cancer, PLoS One 8 (2013) e66165.
[40] Y.X. Lin, F. Yu, N. Gao, J.P. Sheng, J.Z. Qiu, Hu BC. microRNA-143 protects cells from DNA damage-induced killing by downregulating FHIT expression, Cancer Biother. Radiopharm. 26 (2011) 365–372.
[41] T. Iwaya, T. Yokobori, N. Nishida, R. Kogo, T. Sudo, F. Tanaka, et al., Downregulation of miR-144 is associated with colorectal cancer progression via activation of mTOR signaling pathway, Carcinogenesis 33 (2012) 2391–2397.
[42] Y. Hibino, N. Sakamoto, Y. Naito, K. Goto, H.Z. Oo, K. Sentani, et al., Significance of miR-148a in colorectal neoplasia: downregulation of miR-148a contributes to the carcinogenesis and cell invasion of colorectal cancer, Pathobiology 82 (2015) 233–241.
[43] R.K. Jepsen, G.W. Novotny, L.L. Klarskov, I.J. Christensen, L.B. Riis, E. Høgdall, Intra-tumor heterogeneity of microRNA-92a, microRNA-375 and microRNA-424 in colorectal cancer, Exp. Mol. Pathol. 100 (2016) 125–131.
[44] Y. Zhang, X. Hu, X. Miao, K. Zhu, S. Cui, Q. Meng, et al., MicroRNA-425-5p regulates chemoresistance in colorectal cancer cells via regulation of Programmed Cell Death 10, J. Cell. Mol. Med. 20 (2016) 360–369.
[45] P. Hermanek, L. Sobin, TNM Classification of Malignant Tumors, 4th edn., Springer-Verlag, Berlin, 1987, pp. 69–73.
[46] T. Fukui, S. Mori, S. Hatooka, M. Shinoda, T. Mitsudomi, Prognostic evaluation based on a new TNM staging system proposed by the International Association for the Study of Lung Cancer for resected non-small cell lung cancers, J. Thorac. Cardiovasc. Surg. 136 (2008) 1343–1348.
[47] M. Tsukamoto, H. Iinuma, T. Yagi, K. Matsuda, Y. Hashiguchi, Circulating exosomal MicroRNA-21 as a biomarker in each tumor stage of colorectal cancer, Oncology 92 (2017) 360–370.
[48] X. Wu, C.L. Cui, W.L. Chen, Z.Y. Fu, X.Y. Cui, Gong X. miR-144 suppresses the growth and metastasis of laryngeal squamous cell carcinoma by targeting IRS1, Am. J. Transl. Res. 8 (2016) 1–11.
[49] L.Y. Zhang, V. Ho-Fun Lee, A.M. Wong, D.L. Kwong, Y.H. Zhu, S.S. Dong, et al., MicroRNA-144 promotes cell proliferation, migration and invasion in nasopharyngeal carcinoma through repression of PTEN, Carcinogenesis 34 (2013) 454–463.
[50] Y.S. Jia, X.L. Wei, J. Zhao, J.Q. Zheng, Ion channels and tumor, Prog. Physiol. Sci. 38 (2007) 229–234.
[51] D. Vara Ciruelos, M. Dandapani, A. Gray, E.O. Egbani, A.M. Evans, D.G. Hardie, Genotoxic damage activates the AMPK-α1 isoform in the nucleus via Ca2+/CaMKK2 signaling to enhance tumor cell survival, Mol. Cancer Res. 16 (2018) 345–357.